Heliyon 10 (2024) e34311

Contents lists available at ScienceDirect

Heliyon

journal homepage: www.cell.com/heliyon

Research article

Genome-wide analysis of the bZIP gene family in *Cinnamomum camphora* ('Gantong 1') reveals the putative function in anthocyanin biosynthesis

Xiuqi Li [a,b], Xue Gong [b], Hanbin Lin [a,b], Shupei Rao [b], Le Shen [b], Caihui Chen [b], Zhaoxiang Wu [b], Huihu Li [b], Qiaoli Liu [b], Yongda Zhong [a,b,*]

[a] *College of Forestry, Jiangxi Agricultural University, Nanchang, 330045, China*
[b] *Jiangxi Provincial Key Laboratory of Improved Variety Breeding and Efficient Utilization of Native Tree Species, Institute of Biological Resources, Jiangxi Academy of Sciences, Nanchang, 330096, China*

ARTICLE INFO

Keywords:
Anthocyanins
Cinnamomum camphora
bZIP transcription factors

ABSTRACT

Basic leucine zipper (bZIP) transcription factors (TFs) regulate plant development, growth, and secondary metabolism. The formation of red bark of new ornamental cultivar 'Gantong 1' is regulated mainly by anthocyanin anabolism. However, it is unclear whether and which bZIP TFs are involved in this process. We identified 89 genes encoding CcbZIP TFs in *Cinnamomum camphora* genome that could be divided into 14 subfamilies with similar gene structures and conserved motifs. CcbZIP38 and CcbZIP57 were highly conserved compared to HY5 in *Arabidopsis thaliana* and they were highly expressed in the bark and leaves of 'Gantong 1' at different stages. The target gene enrichment analysis showed that indicating indirect involvement of CcbZIP38 and CcbZIP57 in the regulation of anthocyanin synthesis. Our study contributes to understanding the molecular mechanism of anthocyanin synthesis regulation by CcbZIP TFs and provides a theoretical basis for genetic improvement of ornamental traits in *C. camphora*.

1. Introduction

Transcription factors (TFs) are key regulators of eukaryotic gene expression. They activate or inhibit the transcription of target genes by combining with the *cis*-regulatory elements of the promoters during various biological processes [1]. The basic leucine zipper (bZIP) TF family regulates development, growth, secondary metabolism, and responses to stress in plants [2]. The bZIP TF domain consists of 60–80 amino acids, including a highly conserved basic DNA-binding region and a variable leucine zipper region [3]. Hydrophobic forces between hydrophobic amino acids in the leucine zipper region cause dimerization of two bZIP TF molecules that form a hypercoiled structure. In different environments, bZIP monomers of the same or different subfamilies combine to form homo- and heterodimers, respectively, and this dimer diversity expands the number and ability of bZIP dimers to bind target genes [4].

The number of *bZIP* gene families is large, and their functions vary significantly among species. In 2002, Jakoby et al. identified 75 *bZIP* genes in the whole *Arabidopsis thaliana* genome for the first time and divided them into 10 subfamilies [3]. In 2018, Droge-Laser et al. identified 78 *bZIP* TFs in *A. thaliana,* excluding one pseudogene (*AtbZIP73*) and adding four new genes (*AtbZIP76–AtbZIP79*) to the previous list, and divided them into 13 subfamilies [5]. Since then, various *bZIP* TFs have been identified in the genomes of various

* Corresponding author. No. 7777, Changdong Avenue, Gaoxin District, Nanchang, China.
E-mail address: zhongyongda0504@163.com (Y. Zhong).

https://doi.org/10.1016/j.heliyon.2024.e34311
Received 3 July 2024; Accepted 8 July 2024
Available online 10 July 2024

Abbreviations list

bZIP – Basic leucine zipper
CcbZIP – *Cinnamomum camphora* basic leucine zipper
AtbZIP – *Arabidopsis thaliana* basic leucine zipper
TFs – Transcription factors
HY5 – elongated hypocotyl 5
bHLH – basic helix-loop-helix
GBF1 – Golgi Brefeldin A resistant guanine nucleotide exchange factor 1
HYH – HY5 homolog
COP1 – constitutive photomorphogenic 1
GT – 'Gantong 1'
qPCR – Real-time quantitative Polymerase Chain Reaction
MW – Molecular weights
GRAVY – Grand average of hydropathicity
PI – Theoretical isoelectric point
kDa – kilodalton(s)

species, including 92 in *Oryza sativa* [6], 125 in *Zea mays* [7], 77 in *Nicotiana tabacum* [8], and 86 in *Populus trichocarpa* [9].

Anthocyanins are important pigments for plant color, and approximately 80% of the flower color of the angiosperm is determined by anthocyanins [10]. Several studies have shown that bZIP TFs are involved in regulating anthocyanin anabolism in plants. HY5 is a bZIP TF at the center of the transcriptional regulatory network of *A. thaliana*. HY5 regulates anthocyanin biosynthesis by cooperating with MYB TFs such as MYB12, MYB111, and MYB75, or by the synergistic effect with bHLH TF PIF3, which binds to G-box or ACE-box elements in the promoter region of anthocyanin biosynthesis genes, respectively [11]. Meanwhile, GBF1 is a well-known negative regulator of blue light-dependent hypocotyl expansion, but no difference in anthocyanin accumulation was found between wild-type and GBF1 mutant seedlings [12]. Indeed, HY5 and its homolog HYH are degraded in a COP1-dependent manner in the dark, while GBF1 is resolved by different degradation mechanisms, thus largely antagonistic with HY5 and HYH [13]. GBF1 can produce functional interconnection in the form of forming dimer with HY5, and can physically interact with HY5 and HYH in plants [13], and regulate the changes in chlorophyll and anthocyanins content during the growth and development of *Arabidopsis* seedlings. In contrast to HY5, GBF1 and HYH have synergistic effects in chlorophyll and anthocyanins accumulation [12]. When induced by abscisic acid, MdbZIP44 and MdbZIP23 promoted anthocyanin accumulation in red-fleshed apples (*Malus domestica* Borkh.) by enhancing the binding of MdMYB1 and MdNAC1, respectively, to downstream target gene promoters. MdHY5 promoted the accumulation of anthocyanins by regulating the expression of *MdMYB10* and downstream anthocyanin biosynthesis genes [14,15]. Overexpression of *PgbZIP16* and *PgbZIP34* from *Punica granatum* in tobacco promoted the accumulation of anthocyanins in leaves, whereas overexpression of *PgbZIP16* in *A. thaliana* significantly upregulated the expression of anthocyanin synthesis genes, such as *UF3GT*, *ANS*, and *DFR*, and promoted anthocyanin accumulation [16]. bZIP TFs, such as LcABF in *Litchi chinensis* [17], RsbZIP011 and RsbZIP102 in *Raphanus sativus* L. [18], and SlAREB1 in *Solanum lycopersicum* [19], promote the expression of anthocyanin-related genes and accumulation of anthocyanins, whereas *VvbZIP36* is a negative regulator of anthocyanin biosynthesis, as its knockout using CRISPR/Cas9 promoted anthocyanin accumulation in grapevine [20].

Cinnamomum camphora is a representative tree species of subtropical evergreen broad-leaved forests that has an important economic, ecological, and cultural value. As a shade and street tree, *C. camphora* has become one of the main tree species for landscaping in southern China because of its high ornamental value. However, the single-color pattern seriously affects the ornamental value of *C. camphora* and limits its application in landscaping; therefore, breeding colored camphor trees is one of the key goals of plant breeders [21]. The young leaves of the new ornamental cultivar 'Gantong 1' (GT) are orange-red or orange, and the bark of the young branches is light pink with white spots after semi-lignification, and the seasonal changes are obvious. A combined metabolome and transcriptome analysis showed that red color of 'Gantong 1' bark emerges owing to the accumulation of pigments such as pelargonidin, cyanidin, and peonidin-based anthocyanins. Further, "flavonoid biosynthesis" and "phenylpropanoid biosynthesis" pathways were the most significantly enriched pathways in this cultivar [22], but expression levels of bZIP TFs in *C. camphora* has not been examined in detail. Therefore, in this study, we systematically identified *bZIP* gene family members at the genome-wide level and performed phylogenetic and gene structure analysis to analyze their expression profiles in different tissues and organs. We used homologous protein analysis to screen out bZIP TFs that could be related to anthocyanin synthesis and studied their expression patterns in the leaves and bark at different growth stages during the annual growth cycle of 'Gantong 1'. This study lays the foundation for further exploration of how bZIP TFs affect anthocyanin synthesis in *C. camphora* and provides a theoretical basis for further genetic improvement of ornamental *C. camphora* varieties.

2. Materials and methods

2.1. Plant materials

The new *C. camphora* cultivar 'Gantong 1' and the offspring from the same maternal line were used as the control group (CK), were all three-year and planted on the plot of the Jiangxi Academy of Sciences (28°41′52″N, 115°59′31″E) with the same plant growth environment and management. Based on previous observations of leaf and bark color changes over the annual cycle, the leaf and bark samples were taken in January, April, May, July, August, and December 2021 when their color changes were most drastic [21], and stored in a −80 °C ultra-low temperature freezer after flash freezing in liquid nitrogen. Three consecutive samples from three individual plants were mixed as one biological replicate.

2.2. Identification and physicochemical properties of CcbZIPs

The Hidden Markov Model (HMM) file of bZIP TFs (PF00170) was downloaded from the Pfam database (http://pfam.xfam.org/ accessed on November 15, 2022), and 119 possible bZIP transcription factor family members of *C. camphora* were screened by the HMM tools on the HMMER website (https://www.ebi.ac.uk/Tools/hmmer/accessed on December 15, 2022). All members of the *Arabidopsis bZIP* gene family downloaded from the TAIR database (https://www.arabidopsis.org/accessed on December 31, 2022) and 75 putative bZIP TFs family members of *C. camphora* were screened by local BLAST. For sequences with multiple transcripts of the same gene, we selected the transcript with the longest fragment as the representative one. The domains of the *bZIP* gene family protein sequence were verified using NCBI batch CD-Search (https://www. ncbi.nlm.nih.gov/Structure/cdd/wrpsb.cgi/accessed on March 14, 2023) and SMART (http://smart.embl.de/accessed on March 14, 2023). CcbZIPs without the conserved bZIP domain were excluded, and *C. camphora* bZIP TF family members were finally identified after comparative analysis. The physicochemical properties and characteristics of bZIP gene family members in *C. camphora* were calculated by Protparam EXPASY online software (https://web.expasy.org/protparam/accessed on March 28, 2023).

2.3. Phylogenetic analysis of CcbZIPs

To study phylogenetic relationships between bZIP TFs in *C. camphora* and *A. thaliana*, the amino acid sequences of AtbZIP and CcbZIP gene family members were used to construct phylogenetic trees. The MUSCLE module in MAGE11 software was used for sequence alignment, and the neighbor-joining method was used to construct the evolutionary tree according to the sequence alignment results. Bootstrap evaluation of the evolutionary tree was performed with the number of iterations set to 1000 and other parameters left at default values. The obtained evolutionary tree file was saved in the NWK format and entered into the iTOL online website (https://itol.embl.de/itol.cgi/accessed on April 5, 2023).

2.4. Analysis of gene structure, protein conserved motifs, and domains of CcbZIPs

The structure and conserved motifs of the cDNA sequences and corresponding genomic DNA sequences of 89 CcbZIP TFs were analyzed using online software MEME (http://MEME-suite.org/tools/MEME/accessed on April 25, 2023), and the motif was set to 20. Simultaneously, a batch CD search was used to analyze the conserved domains of 89 CcbZIP TF protein sequences in NCBI. TBtools software (https://github.com/CJ-Chen/TBtools/releases accessed on April 26, 2023) was used to visualize gene structure, conserved motifs, and protein domains.

2.5. Collinearity analysis of CcbZIPs

Chromosome localization, length, and density information were extracted from the camphor gene annotation file, and the whole genome and annotation files of *A. thaliana* (GCF_000001735.4), *P. trichocarpa* (GCA_000002775.4), and *C. camphora* (GCA_003546025.1) were extracted from the NCBI website (https://www.ncbi.nlm.nih.gov/genome/accessed on May 30, 2023). Based on the specific members identified, a collinearity analysis was performed using TBtools for three species: *C. camphora*, *P. trichocarpa,* and *A. thaliana.* Simultaneously, the collinear relationships between *C. camphora* and *Cinnamomum kanehirae,* a species related to camphor tree, were analyzed and visualized.

2.6. Expression profiles of CcbZIPs in different tissues

In a previous study, we performed RNA-seq of seven different tissues (stem tips, fruits, roots, xylem, leaves, flowers, and phloem) from *C. camphora* [23]. These data were used to investigate expression patterns of genes encoding CcbZIP TFs. The expression levels of *CcbZIPs* were estimated in fragments per kilobase of transcript per million fragments mapped (FPKM). TBTools software was used to visualize transcriptome FPKM data, and a gene expression heat map was plotted based on $\log_2$ (FPKM).

2.7. Prediction of CcbZIP protein-protein interaction network

A. thaliana protein sequences were queried using STRING online website (https://cn.string-db.org/cgi/accessed on May 10, 2023),

and 89 CcbZIP protein sequences were used as references to predict the protein-protein interaction network.

2.8. Analysis of expression levels of candidate CcbZIP TFs for anthocyanin biosynthesis in cultivar 'Gantong 1'

RNA was extracted from the leaves and bark of 'Gantong 1' and control group with an RNA extraction kit (Huayueyang Biotechnology Co., Ltd., Beijing, China). Total RNA was used as template and reverse transcribed into cDNA using reverse transcription kits (Yisheng Biotechnology Co., Ltd., Shanghai, China). The primers were designed using Primer Premier 5.0 software with Tm values ranging from 55 °C to 60 °C and amplified fragments ranging from 100 to 200 bp in length (Table S1). Primer specificity was verified by semi-quantitative RT-PCR experiments. The fluorescent dye used in real-time quantitative PCR was Hieff UNICON Universal Blue qPCR SYBR Green Master Mix (Yisheng Biotechnology Co., Ltd., Shanghai, China). A two-step qPCR reaction mixture to detect the expression of candidate *CcbZIP* TFs regulating biosynthesis of anthocyanins contained: Hieff UNICON Universal Blue qPCR SYBR Green Master Mix, 10 μL; cDNA(10 ng/μL), 2.0 μL; forward primer (10 μM), 0.4 μL; reverse primer (10 μM), 0.4 μL; and ddH_2O, to 20 μL. Reaction procedure was as follows: 95°C, 30 s, 1 cycle; 95°C, 10 s, 58°C, 30 s, 40 cycles; 95°C, 15 s, 60°C, 1 min, 95°C, 15 s. Gene expression levels were calculated by the $2^{-\Delta\Delta CT}$ method, and actin (*KM086738.1*) was used as internal control [22].

2.9. Identification and annotation of target genes for candidate CcbZIPs

To determine downstream target genes that could be regulated by candidate bZIP TFs, we extracted a 2000 bp promoter sequence of the *C. camphora* gene using TBtools (v2.008). The consensus motif for the bZIP DNA-binding site (MA0551.1) was obtained from the JASPAR database (http://jaspar.genereg.net accessed on November 10, 2023). FIMO program (https://meme-suite.org/meme/doc/fimo.html accessed on November 10, 2023) was used to detect the consensus bZIP binding motif in the *C. camphora* promoter ensemble. Candidate target genes were determined according to the screening criteria of $P < 1 \times 10^{-6}$. The Gene Ontology (GO) and Kyoto Encyclopedia of Genes and Genomes (KEGG) databases (https://magic.novogene.com accessed on November 15, 2023) were used to annotate the functions of candidate bZIP target genes and visualize the results.

3. Results

3.1. Identification of CcbZIPs and determination of their physicochemical properties

Based on the chromosome-level high-quality *C. camphora* genome (GWHBGBX00000000) sequenced in our laboratory, we used the *A. thaliana* bZIP protein sequence as a probe, combined it with the HMM and identified 89 *bZIP* TFs family members (Table S2) named *CcbZIP1–CcbZIP89* according to their chromosomal sequences. The *CcbZIP* genes were unevenly distributed on 12 chromosomes, among which chromosome 4 had the largest number of genes (18), and chromosomes 7 and 10 had the least number of genes (only three each). CcbZIP proteins encoded by these genes ranged from 42 (CcbZIP56) to 919 amino acids in length (CcbZIP30), with molecular weights ranging from 5.12 kD (CcbZIP56) to 101.42 kD (CcbZIP30) and theoretical isoelectric points ranging from 4.92

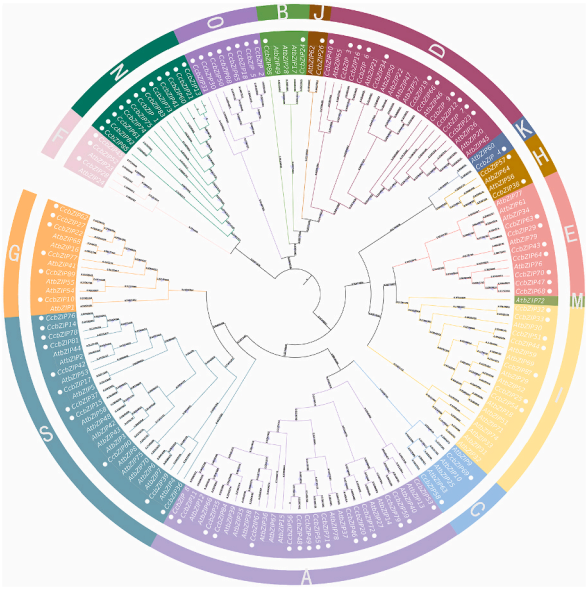

Fig. 1. Phylogenetic relationships of bZIP proteins from *C. camphora* and *A. thaliana* based on the neighbor-joining method. Each subgroup is shown in a different color. The subgroup names and ID numbers are indicated in the outer circle of the phylogenetic tree. (For interpretation of the references to color in this figure legend, the reader is referred to the Web version of this article.)

(CcbZIP04) to 11.5 (CcbZIP39). The GRAVY values of the 89 CcbZIP proteins ranged from −1.068 (CcbZIP38) to −0.049 (CcbZIP30), indicating that all CcbZIP proteins were hydrophilic. The instability indices of CcbZIP proteins ranged from 35.96 (CcbZIP45) to 87.14 (CcbZIP39). Instability indices of only CcbZIP45 and CcbZIP28 were less than 40, indicating that most CcbZIP proteins are unstable.

3.2. Phylogenetic analysis of CcbZIPs

A phylogenetic tree of *C. camphora* was constructed according to the grouping method previously used for the *A. thaliana bZIP* gene family (Fig. 1). Members of the bZIP gene family in *C. camphora* were divided into 14 subfamilies. Subfamilies A, N, and S had the largest numbers of CcbZIP genes, with 15, 13, and 13 members, respectively, whereas the smallest subfamilies, J and K, had only one member each, which was approximately the same as the distribution in *A. thaliana*. In addition, subfamilies O and N were specific to *C. camphora*, being "orphaned" subfamilies, with 8 and 12 members, respectively [21].According to the phylogenetic tree, CcbZIP38 and CcbZIP57 of subfamily H are homologous to the positive phomorphic regulator HY5, and CcbZIP77 of subfamily G is homologous to the negative regulator GBF1 of blue light-dependent hypocotyl expansion, which play important regulatory roles in anthocyanin synthesis.

3.3. Analysis of gene structure, protein conserved motifs, and domains of CcbZIPs

Members of the same subpopulation had the same or similar motif compositions. To better understand the diversity of the composition and structure of the conserved motifs of CcbZIP proteins, we predicted 20 conserved motifs using MEME software. Motif1 is the most common CcbZIP motif, being present in more than 70 % of CcbZIP proteins, but absent in the O and N subfamilies specific to *C. camphora*. Motif13, motif14, motif16, motif17, and motif19 are present only in the O subfamily, whereas motif4 and motif7 occur

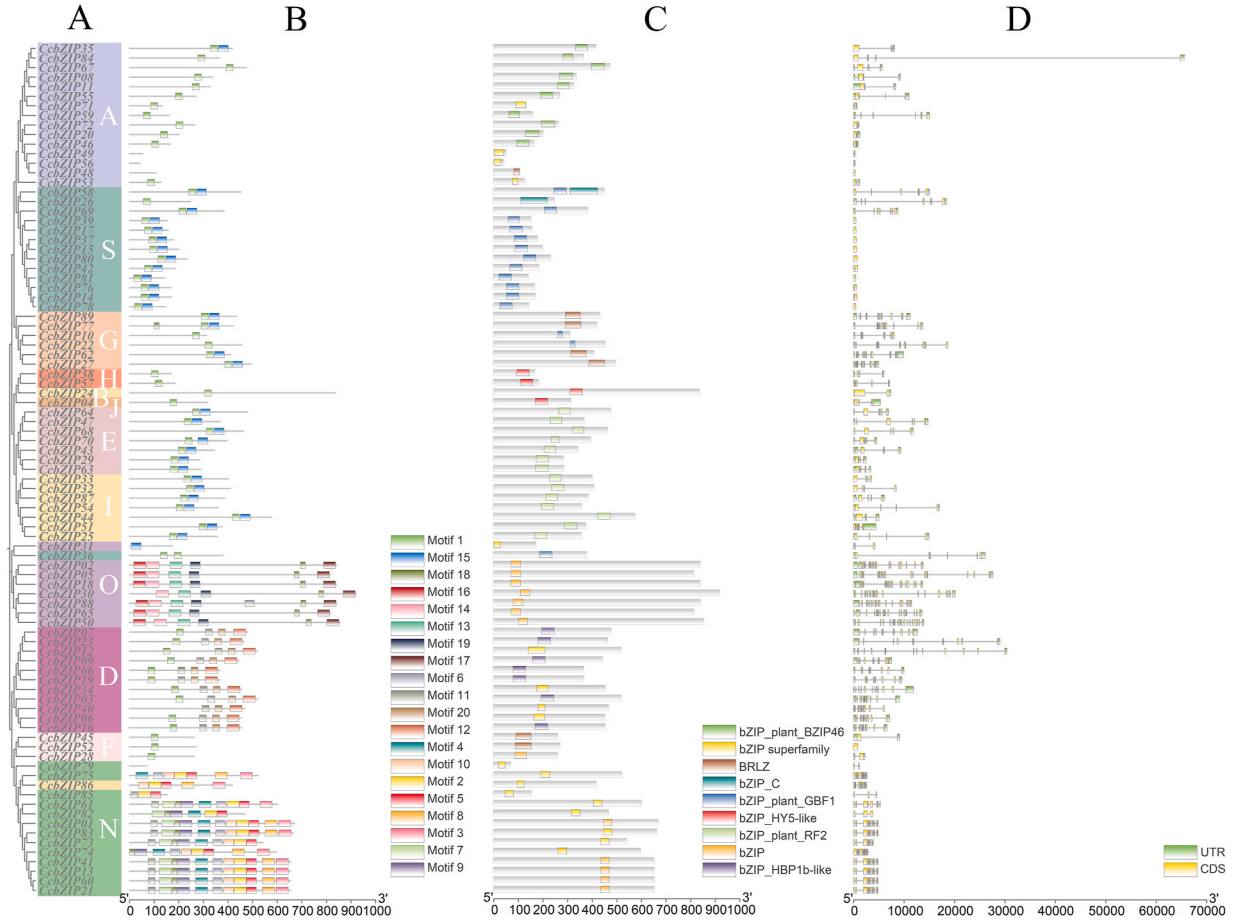

Fig. 2. Conserved motif order, domains, and structure of CcbZIP family member proteins. (A) A phylogenetic tree of 89 CcbZIP proteins was constructed using neighborhood linkage. Different subfamilies are represented by different background colors and labels. (B) Conserved motifs of CcbZIP proteins. Different motifs are represented by squares of different colors; (C) Conserved domains of CcbZIP proteins. (D) Exon-intron structure of *CcbZIP* genes. Coding sequences, introns, and untranslated regions are indicated by yellow boxes, black lines, and green boxes, respectively. (For interpretation of the references to color in this figure legend, the reader is referred to the Web version of this article.)

only in the N subfamily (Fig. 2, Table S3). Domains determine the structural basis of the physiological function of a protein, and a structurally incomplete domain cannot perform a physiological function. Conserved domain analysis showed that all members of the TF family have bZIP protein domains, which belong to multiple small branches under bZIP. The bZIP protein domain is further differentiated according to its biological function and structure, such as bZIP_HY5-like, which is similar to tomato, and *Arabidopsis HY5*, which is a positive regulator of photomorphogenesis.

Gene structure analysis showed that the number and structure of the exons and introns of *CcbZIPs* were highly diverse. The number of exons in the *CcbZIP* genes ranged from 1 to 22, of which five genes (*CcbZIP2, CcbZIP5, CcbZIP30, CcbZIP50, CcbZIP65*) had the largest number of exons (22 each), and nine genes had only one exon (*CcbZIP15, CcbZIP17, CcbZIP37, CcbZIP39, CcbZIP48, CcbZIP52, CcbZIP78, CcbZIP80, CcbZIP81*). *CcbZIP* gene structures were highly conserved and had similar exon-intron structures within the same subfamily.

3.4. Collinearity analysis of CcbZIPs

Chromosomal duplications, tandem repeats, and transposable events are the key means of gene family amplification [24], and a large number of collinear regions can be considered as evidence of genome-wide duplications. The intraspecific genome mapping analysis showed that among the 89 *CcbZIPs*, 35 pairs of genes were fragment duplications, and only two *CcbZIPs* (*CcbZIP7* and *CcbZIP75*) were tandem duplicates on chromosome 10 (Fig. 3). To understand whether *CcbZIPs* were influenced by natural selection during evolution, *Ka/Ks* analyses were performed on tandem and fragment repeat genes. When *Ka/Ks* < 0.5, the gene was considered to have undergone strong purifying selection [25]. For all replicated *CcbZIPs*, *Ka/Ks* values were less than 0.5, indicating that *C. camphora* eliminated deleterious mutations through purifying selection during evolution (Table S4).

Collinear analysis was carried out, and 48 homologous gene pairs were identified between the genomes of *C. camphora* and *A. thaliana*, and 127 between *C. camphora* and *P. trichocarpa* (Fig. 4), indicating that the *CcbZIP* TF family had a closer evolutionary relationship with *P. trichocarpa* than with *A. thaliana*. A total of 138 pairs of homologous genes were found in the collinearity analysis of *C. kanehirae*; however, 19 *CcbZIP* genes were specific to *C. camphora* (Fig. 4). In addition, the *Ka/Ks* values of *bZIP* orthologous genes

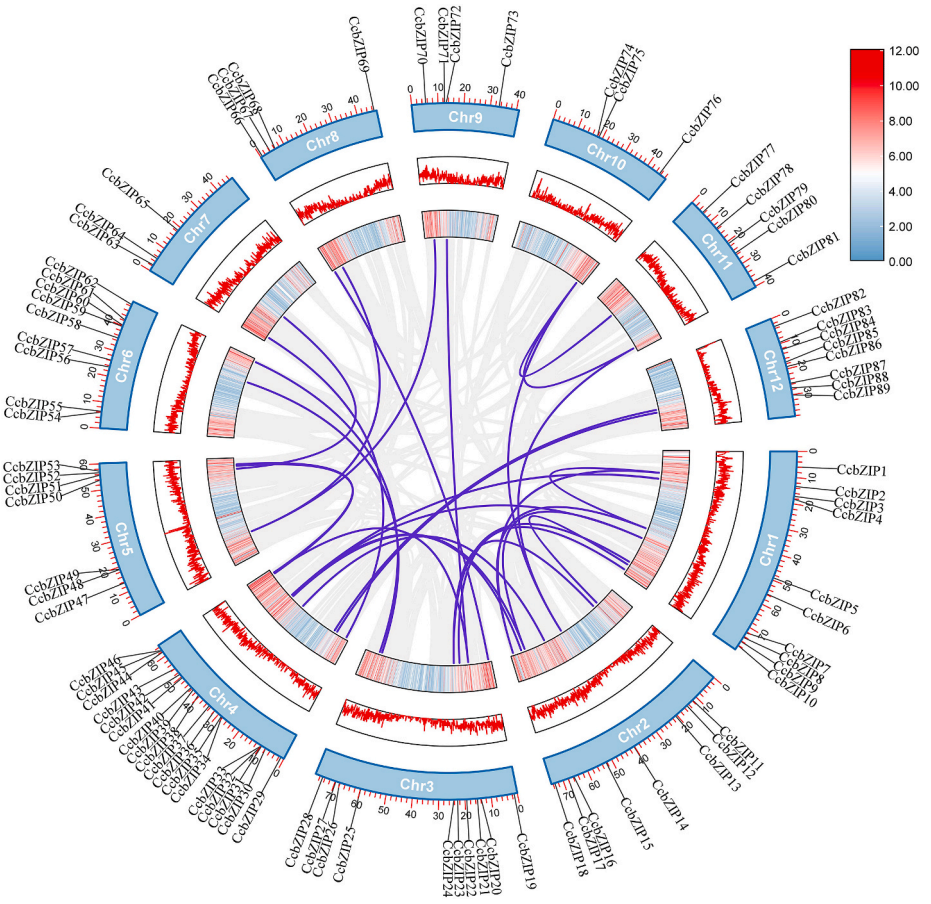

Fig. 3. *CcbZIP* gene family segment duplication events. Segmental repeats in *CcbZIP* genes are linked by blue lines. (For interpretation of the references to color in this figure legend, the reader is referred to the Web version of this article.)

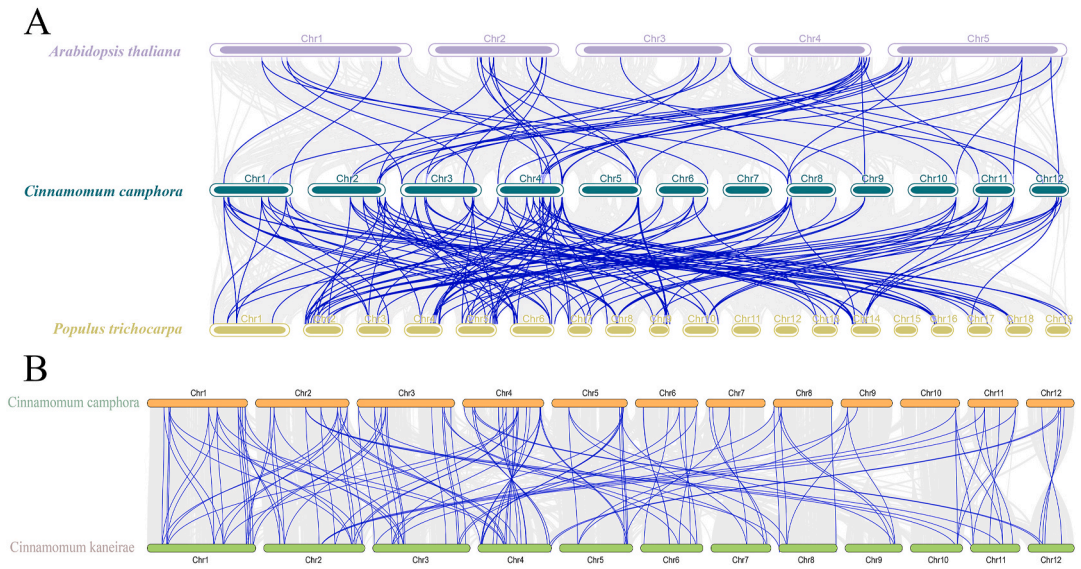

Fig. 4. (A) Collinearity analysis of the bZIP TF family in *C. camphora*, *A. thaliana*, and *P. trichocarpa*. Blue lines link identified collinear genes. (B) Collinearity analysis of the bZIP TFs family in *C. camphora* and *C. kanehirae*. Blue lines link identified collinear genes. (For interpretation of the references to color in this figure legend, the reader is referred to the Web version of this article.)

of *C. camphora*, *A. thaliana,* and *P. trichocarpa* were all less than 1 [26], indicating that the *CcbZIP* gene family underwent strong purifying selection (Tables S5 and S6). Interestingly, eight *CcbZIP* orthologous genes (*CcbZIP11, CcbZIP17, CcbZIP38, CcbZIP43, CcbZIP59* and *CcbZIP80*) in *C. camphora* and *C. kanehirae* had *Ka/Ks* values greater than 1, indicating that these genes underwent strong positive selection and may have evolved recently and rapidly (Table S7).

3.5. Expression profile of CcbZIPs in different tissues

By using hierarchical cluster analysis, we determined expression profiles of *CcbZIPs* in seven different tissues, namely, the roots, stem tips, leaves, xylem, phloem, flowers, and fruits, based on previously published transcriptome data [23]. Expression patterns of *CcbZIPs* significantly varied in different tissues (Fig. 5). Among these, 40, 41, 29, 45, 42, 41, and 44 *CcbZIPs* were highly expressed in the phloem, flowers, leaves, xylem, roots, fruits, and stem tip tissues, respectively (FPKM >10). Twenty-five *CcbZIPs* (*CcbZIP04,*

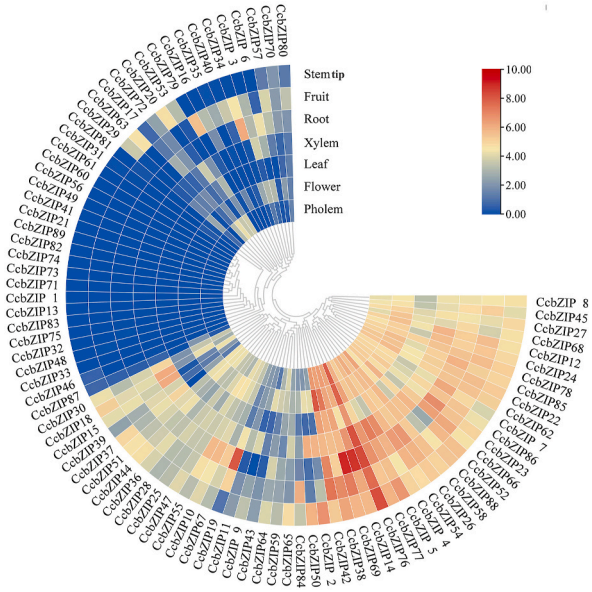

Fig. 5. The heatmap of *CcbZIP* genes in different tissues of *C. camphora* ('Gantong 1'). Scale bars represent the log2 transformations of the fragments per kilobase of transcript per million fragments mapped (FPKM) values.

CcbZIP05, CcbZIP07, CcbZIP12, CcbZIP14, CcbZIP22, CcbZIP23, CcbZIP24, CcbZIP26, CcbZIP27, CcbZIP38, CcbZIP42, CcbZIP45, CcbZIP54, CcbZIP55, CcbZIP58, CcbZIP62, CcbZIP66, CcbZIP68, CcbZIP69, CcbZIP76, CcbZIP77, CcbZIP78, CcbZIP85, and *CcbZIP86*) were highly expressed in all tissues (FPKM >10). Twenty genes (*CcbZIP01, CcbZIP13, CcbZIP21, CcbZIP31, CcbZIP32, CcbZIP33, CcbZIP41, CcbZIP48, CcbZIP49, CcbZIP56, CcbZIP60, CcbZIP61, CcbZIP71, CcbZIP73, CcbZIP74, CcbZIP75, CcbZIP81, CcbZIP82, CcbZIP83* and *CcbZIP89*) were expressed at very low levels or not at all in seven tissues (FPKM <0.5). *CcbZIP76* was the highest in the phloem (FPKM>229), leaves (FPKM>97), xylem (FPKM>284), fruits (FPKM>191), and stem tips (FPKM>302); *CcbZIP42* (FPKM>259) was the highest in the flowers; and *CcbZIP69* (FPKM>520) was the highest in the roots.

3.6. Predicted protein-protein interaction network of CcbZIPs

Using information about *A. thaliana* orthologs of CcbZIPs, we predicted the protein-protein interaction network with STRING online database. Most CcbZIP proteins interacted with each other, and 10 CcbZIP proteins interacted with more than 10 CcbZIP proteins (Fig. S1 and Table S8). The protein-protein interaction network combined with the phylogenetic tree showed that CcbZIP38 was orthologous to HY5, and CcbZIP57 was paralogous to HYH. Being downstream of photosensitizing pigments, cryptochromes, and UV-B photoreceptors, HY5 is involved in many developmental processes, such as photosensitive morphogenesis, chloroplast development, and pigment accumulation. HYH is a homolog of HY5 with partially overlapping functions; it regulates hypocotyl and lateral root growth and pigment accumulation [27,28]. As illustrated in Fig. 6, CcbZIP4/CcbZIP24/CcbZIP38 (HY5) and CcbZIP57 (HYH) work together with TFs such as COP1, PIF3, HFR1, and RUP1 to regulate anthocyanin biosynthesis by affecting the expression of cryptochrome genes (Fig. 6) [29]. These results suggest that TFs such as CcbZIP4, CcbZIP24, CcbZIP38, and CcbZIP57 may be involved in the biosynthesis of anthocyanins in *C. camphora*.

3.7. Analysis of expression levels of candidate CcbZIP TFs for anthocyanin biosynthesis in 'Gantong 1'

To further study the role of CcbZIP TFs in the metabolism and synthesis of anthocyanins in *C. camphora* 'Gantong 1', we used qRT-PCR to verify expression levels of *CcbZIP4*, *CcbZIP14*, *CcbZIP24*, *CcbZIP38*, *CcbZIP42*, *CcbZIP57*, *CcbZIP76* and *CcbZIP77* at different stages of leaf and bark growth and development throughout the annual cycle. In leaves, the expression levels of *CcbZIP4*, *CcbZIP14* and *CcbZIP24* reached their peak in August, but *CcbZIP4* and *CcbZIP24* were significantly lower than those in control trees. An exception was *CcbZIP4* expression level in May, which was higher than that in control trees. At other time periods, was *CcbZIP4* expression level either lower (in December) or essentially the same as that in control trees. *CcbZIP42* and *CcbZIP76* expression levels peaked in December and their expression levels were significantly lower than in control trees in that month; *CcbZIP57* and *CcbZIP77* expression levels peaked in January and their expression levels were higher than control The expression level of *CcbZIP38* peaked in July and remained higher than that in control trees for most of the year, except in December. The expression level of *CcbZIP4* remained lower than that in control trees for most of the year, except in May; The expression of *CcbZIP24* was remained lower than that in control trees for most of the year, except in May and July. The expression level of *CcbZIP57* in the first half of the year was higher than that in the

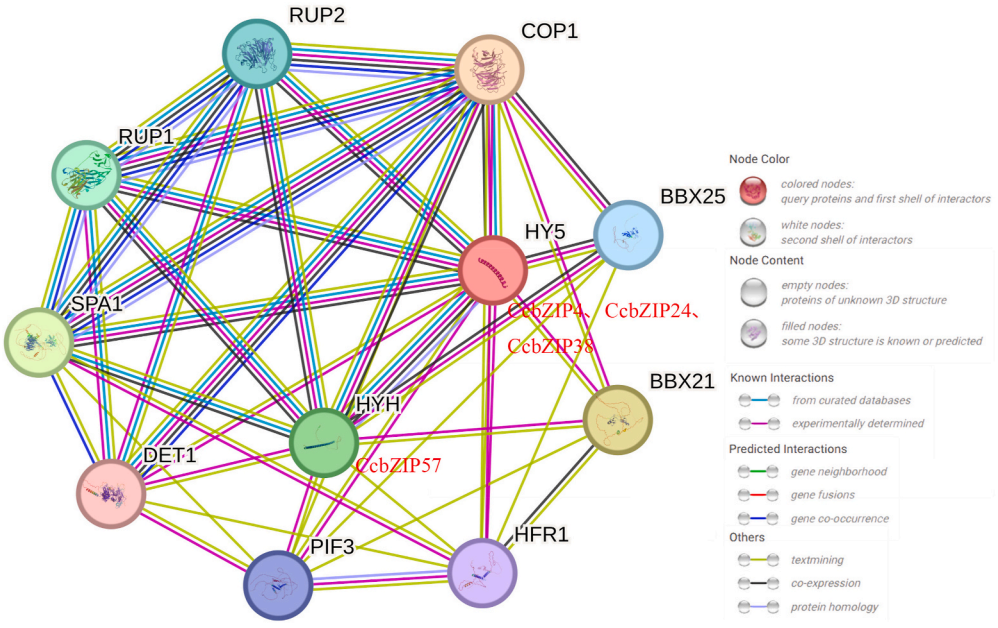

Fig. 6. Predicted protein-protein interaction network of CcbZIP4, CcbZIP24, CcbZIP38, and CcbZIP57 based on the information about their orthologs in *Arabidopsis*.

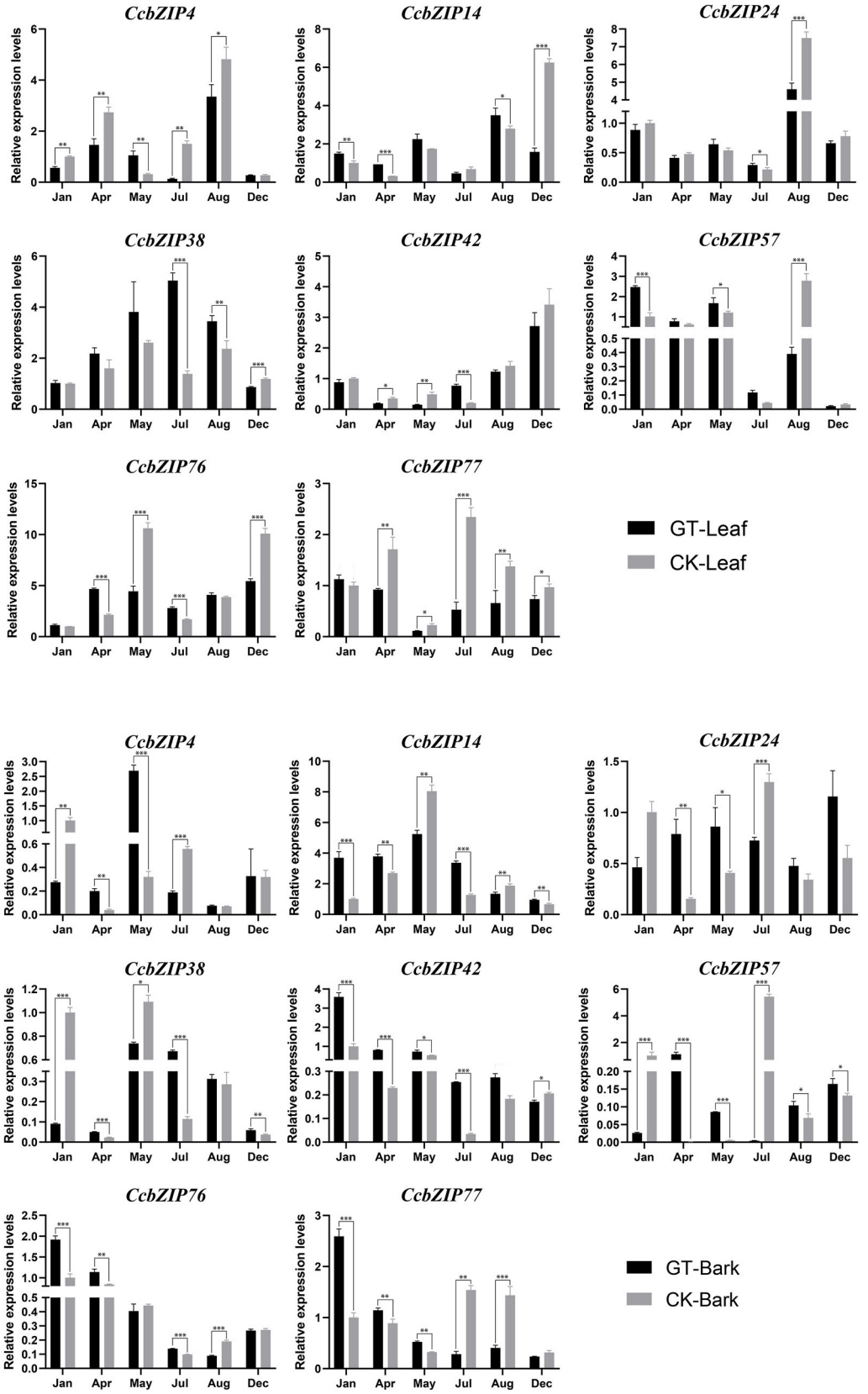

(caption on next page)

Fig. 7. The relative expression of eight transcription factors in the leaves and bark of *C. camphora* cultivar 'Gantong 1' at different stages of development and growth throughout the annual cycle by qRT-PCR. *$P < 0.05$; **$P < 0.01$; ***$P < 0.001$.

control. *CcbZIP57* expression in the first half of the year was higher than that in control trees, but in August, it was significantly lower, whereas in December, it was basically the same as that in control trees. The expression level of *CcbZIP76* remained higher than that in control trees for most of the year, except in May and December,and *CcbZIP77* expression in the second half of the year was lower than that in control trees. All of the eight tested genes expressed in December were lower than the control.

In the bark, the expression of *CcbZIP4*, *CcbZIP24*, *CcbZIP38* and *CcbZIP57* in January in *C. camphora* 'Gantong 1' were lower than that in control trees, and *CcbZIP14*, *CcbZIP42*, *CcbZIP76* and *CcbZIP77* were on the contrary. *CcbZIP4*, *CcbZIP14* and *CcbZIP38* expression levels peaked in May, and the expression of *CcbZIP4* was significantly higher, whereas the expression of *CcbZIP14* and *CcbZIP38* was significantly lower than in control trees.The *CcbZIP14* and *CcbZIP76* expression level in August was significantly lower than that in control trees, which was not the case for expression levels of other six genes. *CcbZIP24* expression levels peaked in December and their expression levels were significantly higher than in control trees in that month. The expression level of *CcbZIP42* remained higher than that in control trees for most of the year, except in December. *CcbZIP42*, *CcbZIP76* and *CcbZIP77* expression levels peaked in January and their expression levels were significantly higher than in control trees in that month. All of the eight tested genes expressed in April were higher than the control. Interestingly, there were significant differences in the expression levels of *CcbZIP57* in January, April, May, and July between 'Gantong 1' and control bark (Fig. 7).

3.8. Identification and annotation of candidate target genes of CcbZIPs

To identify potential downstream target genes regulated by CcbZIP TFs in *C. camphora* and determine their functions, we used the consensus bZIP motif in the JASPAR database to search for a promoter sequence 2.0 kb upstream of the protein-coding gene [30]. In total, 274 target genes were identified for further annotation, of which 94 were annotated using GO. Genes involved in actin binding (GO:0003779), iron-sulfur cluster binding (GO:0051536), metal cluster binding (GO:0051540), and cytoskeletal protein binding (GO:0008092) were significantly enriched ($P < 0.05$), and DNA-binding transcription factor activity (GO:0003700) and transcription regulator activity (GO:0140110) had the highest degree of gene enrichment (Fig. 8). The KEGG results showed that 59 target genes were enriched in 49 pathways. The most representative KEGG functional category was carbon fixation in photosynthetic organisms, followed by photosynthesis, carbon metabolism, glyoxylic acid and dicarboxylic acid metabolism, plant hormone signal transduction, plant circadian rhythm, and carotenoid biosynthesis.

4. Discussion

bZIP TFs are widely distributed in eukaryotes and play important roles in plant growth and development, secondary metabolism,

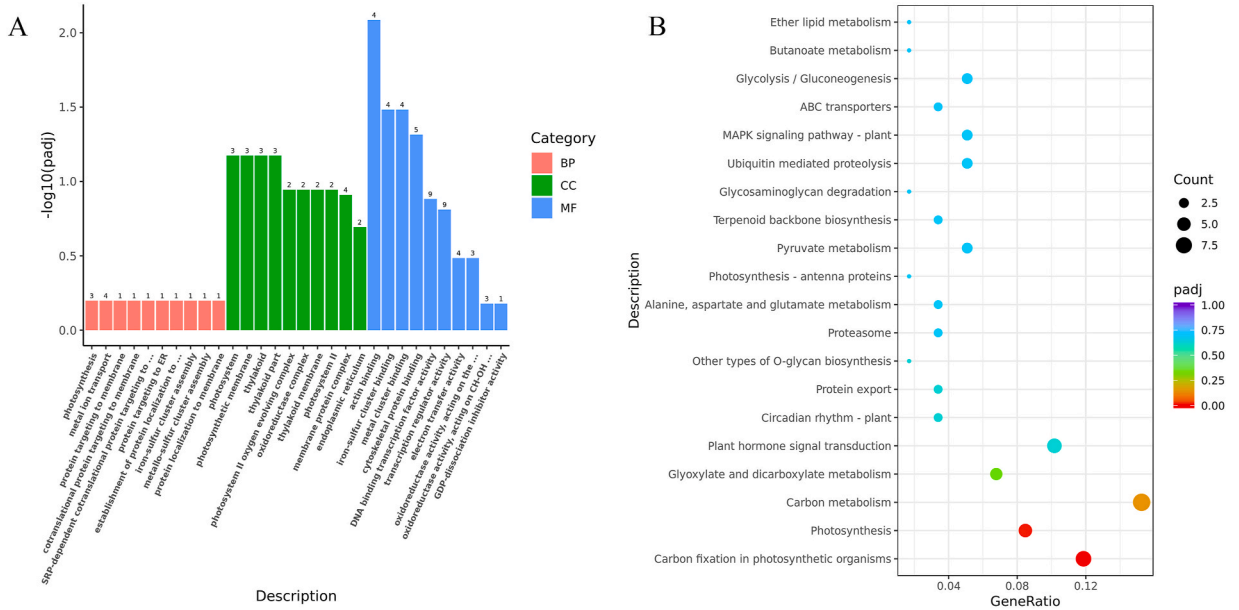

Fig. 8. Two hundred seventy-four target genes downstream of CcbZIP TFs were analyzed using GO (A) and KEGG (B) enrichment analyses. Ratios indicate the level of enrichment, P_{adj} values indicate the confidence level of the results, and size represents the degree of enrichment to the number of genes in the pathway.

and stress responses. The mechanism by which bZIP TFs regulate anthocyanin synthesis has been studied in *A. thaliana*, but how bZIP proteins influence anthocyanin synthesis in woody plants, such as *C. camphora*, is still unclear [5]. In this study, we performed a genome-wide screen for *bZIP* gene family members of *C. camphora.* The number of bZIP TFs in *C. camphora* is comparable to that in *P. trichocarpa* (86) [9] and *Oryza sativa* (92) [6], larger than that in *Nicotiana tabacum* (77) [8] and *A. thaliana* (78) [5], and smaller than that in *Zea mays* (125) [7].

According to the *Arabidopsis* subfamily classification, all CcbZIP TFs were divided into 14 subfamilies, with the largest numbers of members in subfamilies A, N, and S (15, 13, and 13, respectively), which is approximately the same as in *A. thaliana* [5]. In *Arabidopsis*, subfamily A is the largest cluster, mainly involved in the biotic and abiotic stress responses of plants, and plays an important role in resisting drought and salinity-alkali stresses [31–33]. Subfamily S is composed of genes without introns, and the four members of subfamily C, bZIP9, bZIP10, bZIP25, and bZIP63, preferentially isodimerize with S1 members of subfamily S to form the C/S1-bZIP network, which is activated during plant starvation signaling to maintain plant energy homeostasis [34]. Subfamily D increases the survival ability of plants under the stress of pathogenic bacteria and other organisms, and is divided into five evolutionary branches: induction of extracellular defense and endoplasmic reticulum stress response [35], defense response [5], detoxification [36], hormonal interactions between salicylic acid and cytokinin [37], and controlling primordium formation in flower organs [38]. Additionally, subfamily G plays an important role in promoting lateral root development [39] and regulating natural aging [40]. Similar to findings in *A. thaliana*, subfamilies J and K in *C. camphora* contained only one member each, suggesting a relatively slow evolutionary rate and possible functional conservation [41]. For example, AtbZIP60, a member of the subfamily K, is an important regulator of the evolutionarily conserved endoplasmic reticulum stress responses [42]. However, in contrast to the observations in *A. thaliana*, no subfamily M was found in *C. camphora*, which may have been owing to the loss of genes during evolution [43] and the emergence of new subfamilies, N and O, through gene duplication and species divergence.

During plant evolution, more than half of the genes in most plant species consist of repeats, and because of such genetic redundancy, some duplications are preserved during the evolutionary process and allow time for the evolution of new gene functions [43, 44]. Genome-wide duplication events, chromosomal duplications, and tandem duplications may explain the expansion of the bZIP gene family [45]. Previously, we found that 1110 gene families expanded and 1528 gene families contracted in the *C. camphora* genome, of which 163 gene families (2169 genes) experienced rapid expansion and 46 gene families (214 genes) experienced rapid contraction [23]. In addition, genome collinearity analysis of *C. camphora* and other species and analysis of homologous genes in the collinearity region showed that 35 pairs of genes on nine chromosomes had fragment duplications, which may be the main pattern of CcbZIP family expansion. The genome of *C. camphora* underwent three genome-wide duplication events during evolution: the distant whole-genome duplication (WGD) event that was a common event for all angiosperms, an ancient WGD that occurred prior to the differentiation of Laurales and Magnoliales (*Liriodendron chinense*), and a recent WGD event that occurred before the internal differentiation of Laurales [23]. Collinearity analysis of *C. camphora* and *C. kanehirae* also showed that there were some genetic differences between these closely related species as they had different numbers of bZIP TFs. These differences may have been affected by the third internal replication event of Laurales.

Protein-protein interaction analysis can help predict the potential functions of CcbZIP TFs. In this study, we found that CcbZIP38 and CcbZIP57, belonging to subfamily H, are directly homologous to HY5 and HYH, which is a homolog of HY5. Thus, CcbZIP38 and CcbZIP57 may have the same functions as HY5 and HYH, including regulation of anthocyanin biosynthesis. In addition, although CcbZIP4 and CcbZIP24 do not belong subfamily H, they contain the conserved HY5 domain, so they may also be involved in the synthesis of anthocyanins in *C. camphora*. CcbZIP77 is a homolog of GBF1, GBF1 is a long-known, negative regulator of blue-light dependent hypocotyl expansion and thus, performs largely antagonistically to HY5 and HYH [5],and CcbZIP14, CcbZIP42 and CcbZIP76 contain the same domain. However, only a few studies have reported that bZIP TFs directly regulate the expression of downstream structural genes. In *Arabidopsis*, HY5 regulates anthocyanin biosynthesis by acting with MYB TFs, such as MYB12, MYB111, and MYB75, or the bHLH TF PIF3 [11]. Our analysis of CcbZIP targets showed that DNA binding transcription factor activity and transcription regulator activity genes were the most enriched set of genes among putative targets. Genes such as *Ccam05G000916*, *Ccam06G000684*, and *Ccam11G001055* from this set also related to sequence-specific DNA binding (GO:0043565) with respect to their molecular function, but were not directly implicated in the anthocyanin metabolism pathway, suggesting that CcbZIPs may regulate anthocyanin synthesis and metabolism by binding to other TFs. We further verified the expression specificity of eight genes ,including *CcbZIP38*, *CcbZIP57*, *CcbZIP77*,in seven different tissues and their expression levels in leaves and bark at different growth stages during the annual cycle of 'Gantong 1'. Except for *CcbZIP57*, the other seven genes were highly expressed in both the stem tip and phloem, and *CcbZIP4* and *CcbZIP24* were the highest in the phloem, The CcbZIP76 in the eight genes had the highest expression in both leaves and bark,. *CcbZIP4* expression levels in April and May were significantly higher than those in control trees, and *CcbZIP24* expression levels in the leaves in April and May and in the bark in July were significantly higher than those in control trees, respectively. In other periods, *CcbZIP4* and *CcbZIP24* expression levels were lower than those in control trees or equivalent to them; but 'Gantong 1' and control tree phenotypes were similar in the corresponding months, suggesting that *CcbZIP4* and *CcbZIP24* are may not involved in the regulation of anthocyanin synthesis. January is the period when the bark color gap between 'Gantong 1' and the control tree was very obvious, and the expression of *CcbZIP42, CcbZIP76* and *CcbZIP77* reached the highest level in January, and was significantly higher than that of the control tree. Expression levels of *CcbZIP38, CcbZIP57* and *CcbZIP77* in the leaves of 'Gantong 1' and control trees showed significant differences throughout the year. *CcbZIP38* expression levels in the bark were generally higher than those in control trees except in December, when they were significantly lower than in control trees. In turn, *CcbZIP57* expression levels in the bark were higher or basically the same as in control trees except in August, when they were significantly lower than in control trees. *CcbZIP77* expression levels in the leaf were generally lower than those in control trees except in January. The most dramatic phenotypic difference between 'Gantong 1' and control trees is during the first half of the year: the new leaves are red or orange-red, and the branches

are red and densely covered with white spots in contrast to the gray-green stems of the control leaves [21]. These observations indicate that *CcbZIP38*, *CcbZIP57* and *CcbZIP77* may be involved in anthocyanin synthesis.

In this study, we revealed basic characteristics of the *CcbZIP* gene family and predicted related *CcbZIPs* that may regulate the anthocyanin synthesis pathway. This information is valuable for understanding anthocyanin synthesis as well as, more generally, development and growth of *C. camphora*. However, the functions of *CcbZIPs* (*CcbZIP4*, *CcbZIP14*, *CcbZIP24*, *CcbZIP38*, *CcbZIP42*, *CcbZIP57*, *CcbZIP76*, and *CcbZIP77*) require further investigations using transgenic, yeast one-hybrid, etc.

5. Conclusion

In this study, the *bZIP* gene family of *C. camphora* was systematically analyzed for the first time on the genome-wide level. The 89 revealed *CcbZIPs* were unevenly distributed on 12 chromosomes. According to the phylogenetic analysis, they were divided into 14 subfamilies, each of which had similar gene structures and conserved motifs, among which subfamilies N and O were specific to *C. camphora*. The collinearity analysis revealed 35 pairs of fragment repeats in the 89 *CcbZIPs*, and fragment duplication was the primary means of the gene family expansion. Protein-protein interaction network prediction showed that CcbZIP38 and CcbZIP57 were homologous to HY5 and HYH of *A. thaliana*, and their expression levels in cultivar 'Gantong 1' were higher than in control *C. camphora* trees. However, the target gene enrichment analysis showed that the CcbZIP TFs did not directly target anthocyanin biosynthesis genes, indicating that *CcbZIP38* and *CcbZIP57* may regulate anthocyanin synthesis indirectly. Our study provides basic data for the subsequent functional characterization of CcbZIP transcription factors that regulate anthocyanin synthesis in *C. camphora*.

Data availability statement

The chromosome-level high-quality *C. camphora* genome sequence data underlying this study are deposited in the National Genomics Data Center (NGDC) and can be retrieved using the corresponding project number GWHBGBX00000000.

Funding

This research was funded by the National Natural Science Foundation of China (32060354), the Key Industrial Technology Research Project of Jiangxi Academy of Sciences (2021YSBG10002), the Scientific Research Funding of Provincial Talent Training of Jiangxi Academy of Sciences (2023YRCS004), and National Government Guidance Fund for Regional Science and Technology Development (20192ZDD01004).

CRediT authorship contribution statement

Xiuqi Li: Conceptualization, Investigation, Software, Validation, Visualization, Writing – original draft. **Xue Gong:** Methodology, Resources. **Hanbin Lin:** Methodology, Validation, Visualization. **Shupei Rao:** Validation, Writing – review & editing. **Le Shen:** Resources, Software. **Caihui Chen:** Resources, Validation, Writing – review & editing. **Zhaoxiang Wu:** Formal analysis, Resources. **Huihu Li:** Formal analysis. **Qiaoli Liu:** Resources. **Yongda Zhong:** Conceptualization, Funding acquisition, Resources, Supervision, Writing – review & editing.

Declaration of competing interest

The authors declare the following financial interests/personal relationships which may be considered as potential competing interests:Yongda Zhong reports financial support was provided by National Natural Science Foundation of China. Yongda Zhong reports financial support, administrative support, and equipment, drugs, or supplies were provided by Jiangxi Academy of Sciences. If there are other authors, they declare that they have no known competing financial interests or personal relationships that could have appeared to influence the work reported in this paper.

Appendix A. Supplementary data

Supplementary data to this article can be found online at https://doi.org/10.1016/j.heliyon.2024.e34311.

References

[1] S. Kong, S.Y. Park, Y.H. Lee, Systematic characterization of the bZIP transcription factor gene family in the rice blast fungus, *Magnaporthe oryzae*, Environ. Microbiol. 17 (4) (2015) 1425–1443, https://doi.org/10.1111/1462-2920.12633.

[2] H. Han, C. Wang, X. Yang, et al., Role of bZIP transcription factors in the regulation of plant secondary metabolism, Planta 258 (1) (2023) 13, https://doi.org/10.1007/s00425-023-04174-4.

[3] M. Jakoby, B. Weisshaar, W. Dröge-Laser, et al., bZIP transcription factors in *Arabidopsis*, Trends Plant Sci. 7 (3) (2002) 106–111, https://doi.org/10.1016/s1360-1385(01)02223-3.

[4] J.A. Rodriguez-Martinez, A.W. Reinke, D. Bhimsaria, A.E. Keating, A.Z. Ansari, Combinatorial bZIP dimers display complex DNA-binding specificity landscapes, Elife 6 (6) (2017), https://doi.org/10.7554/eLife.19272.

[5] W. Droge-Laser, B.L. Snoek, B. Snel, C. Weiste, The *Arabidopsis* bZIP transcription factor family-an update, Curr. Opin. Plant Biol. 45 (Pt A) (2018) 36–49, https://doi.org/10.1016/j.pbi.2018.05.001.

[6] A. Nijhawan, M. Jain, A.K. Tyagi, J.P. Khurana, Genomic survey and gene expression analysis of the basic leucine zipper transcription factor family in rice, Plant Physiol 146 (2) (2007) 323–324, https://doi.org/10.1104/pp.107.112821.

[7] K. Wei, J. Chen, Y. Wang, et al., Genome-wide analysis of bZIP-encoding genes in maize, DNA Res. 19 (6) (2012) 463–476, https://doi.org/10.1093/dnares/dss026.

[8] L. Duan, Z. Mo, Y. Fan, et al., Genome-wide identification and expression analysis of the bZIP transcription factor family genes in response to abiotic stress in *Nicotiana tabacum* L, BMC Genom. 23 (1) (2022) 318, https://doi.org/10.1186/s12864-022-08547-z.

[9] K. Zhao, S. Chen, W. Yao, Z. Cheng, B. Zhou, T. Jiang, Genome-wide analysis and expression profile of the bZIP gene family in poplar, BMC Plant Biol. 21 (1) (2021) 122, https://doi.org/10.1186/s12870-021-02879-w.

[10] Y. Zhao, C. Jiang, J. Lu, Y. Sun, Y. Cui, Research progress of proanthocyanidins and anthocyanidins, Phytother Res. 37 (6) (2023) 2552–2577, https://doi.org/10.1002/ptr.7850.

[11] S.N. Gangappa, J.F. Botto, The multifaceted roles of HY5 in plant growth and development, Mol. Plant 9 (10) (2016) 1353–1365, https://doi.org/10.1016/j.molp.2016.07.002.

[12] C. Mallappa, V. Yadav, P. Negi, S. Chattopadhyay, A basic leucine zipper transcription factor, G-box-binding factor 1, regulates blue light-mediated photomorphogenic growth in *Arabidopsis*, J. Biol. Chem. 281 (31) (2006) 22190–22199, https://doi.org/10.1074/jbc.m601172200.

[13] A. Singh, H. Ram, N. Abbas, S. Chattopadhyay, Molecular interactions of GBF1 with HY5 and HYH proteins during light-mediated seedling development in Arabidopsis thaliana, J. Biol. Chem. 287 (31) (2012) 25995–26009, https://doi.org/10.1074/jbc.m111.333906.

[14] J.P. An, F.J. Qu, J.F. Yao, et al., The bZIP transcription factor MdHY5 regulates anthocyanin accumulation and nitrate assimilation in apple, Hortic. Res. 4 (2017) 17023, https://doi.org/10.1038/hortres.2017.23.

[15] W. Liu, Z. Mei, L. Yu, et al., The ABA-induced NAC transcription factor MdNAC1 interacts with a bZIP-type transcription factor to promote anthocyanin synthesis in red-fleshed apples, Hortic. Res. 10 (5) (2023) uhad49, https://doi.org/10.1093/hr/uhad049.

[16] S. Wang, X. Zhang, B. Li, X. Zhao, Y. Shen, Z. Yuan, Genome-wide identification and characterization of bZIP gene family and cloning of candidate genes for anthocyanin biosynthesis in pomegranate (*punica granatum*), BMC Plant Biol. 22 (1) (2022) 170, https://doi.org/10.1186/s12870-022-03560-6.

[17] B. Hu, B. Lai, D. Wang, et al., Three LcABFs are involved in the regulation of chlorophyll degradation and anthocyanin biosynthesis during fruit ripening in *Litchi chinensis*, Plant Cell Physiol. 60 (2) (2019) 448–461, https://doi.org/10.1093/pcp/pcy219.

[18] L. Fan, L. Xu, Y. Wang, M. Tang, L. Liu, Genome- and transcriptome-wide characterization of bZIP gene family identifies potential members involved in abiotic stress response and anthocyanin biosynthesis in radish (R*aphanus sativus* L.), Int. J. Mol. Sci. 20 (24) (2019) 6334, https://doi.org/10.3390/ijms20246334.

[19] Z. Xu, J. Wang, Y. Ma, et al., The bZIP transcription factor SlAREB1 regulates anthocyanin biosynthesis in response to low temperature in tomato, Plant J. 115 (1) (2023) 205–219, https://doi.org/10.1111/tpj.16224.

[20] M. Tu, J. Fang, R. Zhao, et al., CRISPR/Cas9-mediated mutagenesis of *Vvbzip36* promotes anthocyanin accumulation in grapevine (*Vitis vinifera*), Hortic. Res. 9 (2022) uhac022, https://doi.org/10.1093/hr/uhac022.

[21] X. Gong, T. Shen, X. Li, et al., Genome-wide characterization and analysis of bHLH transcription factors related to anthocyanin biosynthesis in *Cinnamomum camphora* ('Gantong 1'), Int. J. Mol. Sci. 24 (4) (2023), https://doi.org/10.3390/ijms24043498.

[22] Y. Zhong, C. Chen, X. Gong, et al., Transcriptome and metabolome analyses reveal a key role of the anthocyanin biosynthetic pathway cascade in the pigmentation of a *Cinnamomum camphora* red bark mutant ('Gantong 1'), Ind. Crop. Prod. 175 (2022) 114236, https://doi.org/10.1016/j.indcrop.2021.114236.

[23] T. Shen, H. Qi, X. Luan, et al., The chromosome-level genome sequence of the camphor tree provides insights into Lauraceae evolution and terpene biosynthesis, Plant Biotechnol. J. 20 (2) (2022) 244–246, https://doi.org/10.1111/pbi.13749.

[24] C. Maher, L. Stein, D. Ware, Evolution of *Arabidopsis* microRNA families through duplication events, Genome Res. 16 (4) (2006) 510–519, https://doi.org/10.1101/gr.4680506.

[25] Z. Wang, K. Cheng, L. Wan, et al., Genome-wide analysis of the basic leucine zipper (bZIP) transcription factor gene family in six legume genomes, BMC Genom. 16 (2015) 1053, https://doi.org/10.1186/s12864-015-2258-x.

[26] Z. Yang, J.P. Bielawski, Statistical methods for detecting molecular adaptation, Trends Ecol. Evol. 15 (12) (2000) 496–503, https://doi.org/10.1016/s0169-5347(00)01994-7.

[27] R. Sibout, P. Sukumar, C. Hettiarachchi, M. Holm, G.K. Muday, C.S. Hardtke, Opposite root growth phenotypes of *hy5* versus *hy5 hyh* mutants correlate with increased constitutive auxin signaling, PLoS Genet. 2 (11) (2006) e202, https://doi.org/10.1371/journal.pgen.0020202.

[28] Y. Yang, T. Liang, L. Zhang, et al., UVR8 interacts with WRKY36 to regulate *HY5* transcription and hypocotyl elongation in *Arabidopsis*, Nat. Plants 4 (2) (2018) 98–107, https://doi.org/10.1038/s41477-017-0099-0.

[29] N. Tissot, R. Ulm, Cryptochrome-mediated blue-light signalling modulates UVR8 photoreceptor activity and contributes to UV-B tolerance in Arabidopsis, Nat. Commun. 11 (1) (2020) 1323, https://doi.org/10.1038/s41467-020-15133-y.

[30] B. Huang, Z. Huang, R. Ma, et al., Genome-wide identification and expression analysis of LBD transcription factor genes in Moso bamboo (*Phyllostachys edulis*), BMC Plant Biol. 21 (1) (2021) 296, https://doi.org/10.1186/s12870-021-03078-3.

[31] R.R. Finkelstein, T.J. Lynch, The Arabidopsis abscisic acid response gene *ABI5* encodes a basic leucine zipper transcription factor, Plant, Cell 12 (4) (2000) 599–609, https://doi.org/10.1105/tpc.12.4.599.

[32] A. Banerjee, A. Roychoudhury, Abscisic-acid-dependent basic leucine zipper (bZIP) transcription factors in plant abiotic stress, Protoplasma 254 (1) (2017) 3–16, https://doi.org/10.1007/s00709-015-0920-4.

[33] T. Yoshida, J. Mogami, K. Yamaguchi-Shinozaki, Omics approaches toward defining the comprehensive abscisic acid signaling network in plants, Plant Cell Physiol. 56 (6) (2015) 1043–1052, https://doi.org/10.1093/pcp/pcv060.

[34] W. Dröge-Laser, C. Weiste, The C/S1 bZIP Network: a regulatory hub orchestrating plant energy homeostasis, Trends Plant Sci. 23 (5) (2018) 422–433, https://doi.org/10.1016/j.tplants.2018.02.003.

[35] L. Wang, P.R. Fobert, *Arabidopsis* Clade I TGA factors regulate apoplastic defences against the bacterial pathogen *Pseudomonas syringae* through endoplasmic reticulum-based processes, PLoS One 8 (9) (2013) e77378, https://doi.org/10.1371/journal.pone.0077378.

[36] S. Mueller, B. Hilbert, K. Dueckershoff, et al., General detoxification and stress responses are mediated by oxidized lipids through TGA transcription factors in *Arabidopsis*, Plant Cell 20 (3) (2008) 768–785, https://doi.org/10.1105/tpc.107.054809.

[37] J. Choi, S.U. Huh, M. Kojima, H. Sakakibara, K.H. Paek, I. Hwang, The cytokinin-activated transcription factor ARR2 promotes plant immunity via TGA3/NPR1-dependent salicylic acid signaling in *Arabidopsis*, Dev. Cell 19 (2) (2010) 284–295, https://doi.org/10.1016/j.devcel.2010.07.011.

[38] A.T. Maier, S. Stehling-Sun, S.L. Offenburger, J.U. Lohmann, The bZIP transcription factor PERIANTHIA: a multifunctional hub for meristem control, Front. Plant Sci. 2 (2011) 79, https://doi.org/10.3389/fpls.2011.00079.

[39] J.P. Maurya, V. Sethi, S.N. Gangappa, N. Gupta, S. Chattopadhyay, Interaction of MYC2 and GBF1 results in functional antagonism in blue light-mediated Arabidopsis seedling development, Plant J. 83 (3) (2015) 439–450, https://doi.org/10.1111/tpj.12899.

[40] A. Smykowski, P. Zimmermann, U. Zentgraf, Correction. G-box binding Factor1 reduces *CATALASE2* expression and regulates the onset of leaf senescence in Arabidopsis, Plant Physiol 170 (2) (2016) 1164–1167, https://doi.org/10.1104/pp.16.00050.

[41] Y. Fang, J. Jiang, X. Hou, et al., Plant protein-coding gene families: their origin and evolution, Front. Plant Sci. 13 (2022) 995746, https://doi.org/10.3389/fpls.2022.995746.

[42] K. Kanehara, Y. Cho, C.Y. Yu, A lipid viewpoint on the plant endoplasmic reticulum stress response, J. Exp. Bot. 73 (9) (2022) 2835–2847, https://doi.org/10.1093/jxb/erac063.

[43] N. Panchy, M. Lehti-Shiu, S. Shiu, Evolution of gene duplication in plants, Plant Physiol 171 (4) (2016) 2294–2316, https://doi.org/10.1104/pp.16.00523.
[44] J. Zhang, Genetic redundancies and their evolutionary maintenance, Adv. Exp. Med. Biol. 751 (2012) 279–300, https://doi.org/10.1007/978-1-4614-3567-9_13.
[45] Y. Zhou, D. Xu, L. Jia, et al., Genome-wide identification and structural analysis of bZIP transcription factor genes in *Brassica napus*, Genes 8 (10) (2017) 288, https://doi.org/10.3390/genes8100288.